SOUND MORPHOLOGIES DUE TO NON-LINEAR INTERACTIONS: TOWARDS A PERCEPTUAL CONTROL OF ENVIRONMENTAL SOUND SYNTHESIS PROCESSES

Samuel Poirot, Stefan Bilbao, Mitsuko Aramaki, Richard Kronland-Martinet

HAL Id: hal-01881353

https://ensta-paris.hal.science/hal-01881353

Submitted on 25 Sep 2018

SOUND MORPHOLOGIES DUE TO NON-LINEAR INTERACTIONS : TOWARDS A PERCEPTUAL CONTROL OF ENVIRONMENTAL SOUND SYNTHESIS PROCESSES

Samuel Poirot

Aix Marseille Univ, CNRS, PRISM, Marseille, France
`poirot@prism.cnrs.fr`

Stefan Bilbao

Acoustics and Audio Group, James Clerk Maxwell Building, University of Edinburgh, EH9 3JZ, Edinburgh, United Kingdom
`s.bilbao@ed.ac.uk`

Mitsuko Aramaki

Aix Marseille Univ, CNRS, PRISM, Marseille, France
`aramaki@prism.cnrs.fr`

Richard Kronland-Martinet

Aix Marseille Univ, CNRS, PRISM, Marseille, France
`kronland@prism.cnrs.fr`

ABSTRACT

This paper is concerned with perceptual control strategies for physical modeling synthesis of vibrating resonant objects colliding non-linearly with rigid obstacles. For this purpose, we investigate sound morphologies from samples synthesized using physical modeling for non-linear interactions. As a starting point, we study the effect of linear and non-linear springs and collisions on a single-degree-of-freedom system and on a stiff strings. We then synthesize realistic sounds of a stiff string colliding with a rigid obstacle. Numerical simulations allowed the definition of specific signal patterns characterizing the non linear behavior of the interaction according to the attributes of the obstacle. Finally, a global description of the sound morphology associated with this type of interaction is proposed. This study constitutes a first step towards further perceptual investigations geared towards the development of intuitive synthesis controls.

1. INTRODUCTION

This paper is concerned with the perceptual control of environmental sound synthesis processes, based on the ecological approach to auditory events [1],[2]. This approach, adapted from the ecological approach to visual perception [3], supposes the existence of invariant structures (specific patterns in the perceived signal) that carry the necessary information for the recognition of sound events. These structures can be split in two groups: the structural invariants, which enable the recognition of properties of a sounding object and transformational invariants, that describe the transformations of the object. This theory was first exploited by Warren and Verbrugge concerning the auditory recognition of acoustic events [4]. Then, some studies have identified invariants containing sufficient information to discriminate the material [5] or the size [6] of impacted objects. More recently, This approach has inspired a conceptual description of sounds through an action-object paradigm [7],[8],[9].

Research into sound invariants is of great interest for the perceptual control of sound synthesis. Indeed, the definition of a morphology corresponding to an invariant allows for simplified control through the mapping of several synthesis parameters to one global parameter described perceptually. Thus, it allows for the control of sound synthesis processes using high level descriptors, according to perceptual measures.

This conceptual description has led synthesis processes based on the source-filter model. In [7],[8],[9] transformational invariants are responsible for the evocation of a sound-producing action (scratching, rolling), while structural invariants are responsible for the evocation of the exited object (shape, material, size). Hence, in the source-filter model the resulting sound is obtained by the convolution between the transformational invariant defining the source (action) and the structural invariant defining the filter (object).

One aim here is to develop new tools for sound designers, giving them an alternative to databases of recorded sounds for different applications such as video games. It leads to real-time synthesis of sounds in virtual or augmented reality environments directly controlled by the in-game events. In contrast to methods based on the use of a database of recorded sounds, such a synthesis procedure can adapt quickly to event occuring during gameplay. Also, it opens the perspective of generating unheard sounds that carry information contained in the sound invariants: "sound metaphors".

In previous studies, the mapping of perceptual features onto synthesis parameters for an intuitive control of sounds has been proposed [10]. Aramaki et al. developed an impact sound synthesizer intuitively controlled with semantic labels describing the perceived material, size and shape of the object [11],[12]. Here, the authors defined several labeled structural invariants (material, size and shape) in relation to signal properties (modes, damping). The impact synthesizer was extended to continuous-interaction sounds: rubbing, scratching, and rolling [9]. Here, transformational invariants are characterized as a statistical description of the excitation signal in relation to the perceived action. Also, Thoret et al. proposed a description of the non-linear transitions between squeaks and self-oscillation [13].

The aim of this study is to define the invariants relative to the disturbance undergone by a vibrating resonant object when it collides with a non-resonant obstacle. This kind of interaction are a regular occurrence in daily life. For example, in the case of electronic vibrating objects, one can hear a "buzzy" sound whenever they touch a stiff obstacle (washing machine, microwave, vibrating phone...). It occurs as well in various acoustic musical instruments. For instance, the particular timbre of the tanpura results from the collisions between the strings and the bridge [14]. Also, guitarists can produce a screaming tone by playing a pinched harmonic, and a large range of sounds can be generated using prepared pianos [15]. We can see here that this type of interaction includes a wide

range of phenomena from a perceptual point of view. Indeed, we perceive a vibrating phone on a table as a sequence of impacts, a natural harmonic on a string produces a short "buzzy" sound followed by a new modal state of the string, and in some other cases, it may produce harmonic distortion, affect the sustain, the modes' frequency or even change the type of interaction (e.g., transition from squeak to self-oscillation on a glass).

As a first step towards define these invariants, we consider a 1-D resonant object (a stiff string) colliding with a clamped stiff obstacle not located too close to the string ends. This would correspond to the action of choking a string or playing a natural harmonic if the obstacle is located at a specific position. In this case, there is no possible coupling between the string and the barrier as both of them are clamped to the ground and we do not study the specific behavior when the obstacle is close to the bridge.

There are recent investigations into the numerical modeling of collisions in musical instruments [16][17], but very little work on the perceptual characterization of the synthesized signal.

Our approach consists in first gathering a database representative of the diversity of sounds that can be produced with this type of interaction. We made the choice here to synthesize samples using a numerical solving of the differential equations that describe the physical behavior of the system, as it allows the synthesis of realistic sounds with a precise control over all the experimental parameters. We then propose an empirical description of the signal related to the type of interaction. Finally, we make hypotheses regarding the signal elements that seem to be significant for the perception of the phenomena to characterize the related sound invariant.

The next step is to validate these hypotheses through listening tests that consist in comparing reference sounds synthesised with the physical model to sounds synthesized with a signal model reproducing precisely the sound morphologies that seem to be important for the perception of the phenomena according to our observations. The sounds will be synthesized to evoke different spatial locations and structure of the obstacle.

Also, we may expand our study to include interactions close to the string ends (e.g. tanpura), with coupling between the objects (e.g. rattling elements) and apply these sound invariants to any type of objects (shape, material and size). This will lead to other perceptual tests and, it is hoped, to a real-time synthesis process controlled by perceptual features according to the action-object conceptual description of sounds. The final aim is to improve the design of the source-filter synthesis process and the related conceptual description of sounds to include this new type of interaction.

This article is organized as follows: To introduce how non-linear interactions modify the response of a system, a brief overview of the effects of non-linear springs and collisions on a single-degree-of-freedom system is presented in the next section. The following section details the effect of springs and collisions on a stiff string, and a description of signal morphology is proposed subsequently. Conclusions and perspectives are presented in the last section.

Sound examples are available at `https://drive.google.com/open?id=1sNUu6krfWO-rCZD_vJV4SrZ4RUyloJfq`

2. NON-LINEAR SPRINGS AND COLLISIONS ON A SINGLE DEGREE-OF-FREEDOM SYSTEM

In this section, we aim to describe the effects of collisions on the signal morphology for the simplest vibrating system: a 1 Degree-of-Freedom (DoF) mass/spring/damper system. This is the first step to understand how the signal is affected by collisions on a rigid barrier.

2.1. Single degree-of-freedom system

Consider a mechanical damped harmonic oscillator, of mass M, stiffness K_0 and damping constant σ_0, and with displacement $u(t)$ as a function of time t. The ordinary differential equation governing the displacement of the oscillator is

$$\frac{d^2u}{dt^2} = -\omega_0^2 u - 2\sigma_0 \frac{du}{dt} \tag{1}$$

where $\omega_0 = \sqrt{K_0/M}$. For underdamped conditions (as is usually the case in musical systems), the general solution is

$$u(t) = e^{-\sigma_0 t} \left(A\cos(\omega t) + B\sin(\omega t) \right) \tag{2}$$

where $\omega = \sqrt{\omega_0^2 - \sigma_0^2}$, and for some constants A and B determined by initial conditions.

In discrete time, consider the time series u^n, representing an approximation to $u(t)$ at time $t = nk$, where k is the time step (and $F_s = 1/k$ is the associated sample rate). An explicit finite difference scheme approximating (6) above may be written, in condensed operator form, as:

$$\delta_{tt} u^n = -\omega_0^2 u^n - 2\sigma_0 \delta_{t\cdot} u^n \tag{3}$$

where

$$\delta_{tt} u^n = \frac{1}{k^2} \left(u^{n+1} - 2u^n + u^{n-1} \right), \, \delta_{t\cdot} u^n = \frac{1}{2k} \left(u^{n+1} - u^{n-1} \right) \tag{4}$$

This scheme may be written more explicitly as a recursion allowing the calculation of u^{n+1} from u^n and u^{n-1}:

$$u^{n+1} = (u^n(2 - k^2\omega^2) + u^{n-1}(-1 + k\sigma_0))/(1 + k\sigma_0) \tag{5}$$

2.2. Effect of a non-linear spring

As we model the barrier as a unilateral non-linear spring, it is of interest to take a look at a classic non-linear spring (see figure1):
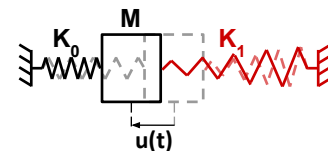

Figure 1: *Damped harmonic oscillator with a cubic spring of stiffness coefficient K_1.*

$$\frac{d^2u}{dt^2} = -\omega_0^2 u - 2\sigma_0 \frac{du}{dt} - H(t - t_0)\omega_1^4 u^3 \tag{6}$$

With $\omega_1 = \sqrt[4]{\frac{K_1}{M}}$, K_1 the stiffness of the cubic spring, $H(t)$ the Heaviside step function, and t_0 the time of appearance of the non-linear spring (here, we set $t_0 = 1s$).

We solve the problem with the following scheme[18]:

$$\delta_{tt}u^n = -\omega_0^2 u^n - 2\sigma_0 \delta_t. u^n - H[n - \frac{t_0}{k}]\omega_1^4 (u^n)^2 \mu_t. u \quad (7)$$

with $\mu_t. u = (u^{n+1} + u^{n-1})/2$, $H[n]$ the discrete Heaviside step function.

The appearance of the non-linear part in a second time allows us to visualise the linear behavior (for $t < t_0$) and the non-linear behavior ($t > t_0$) on the same spectrogram.
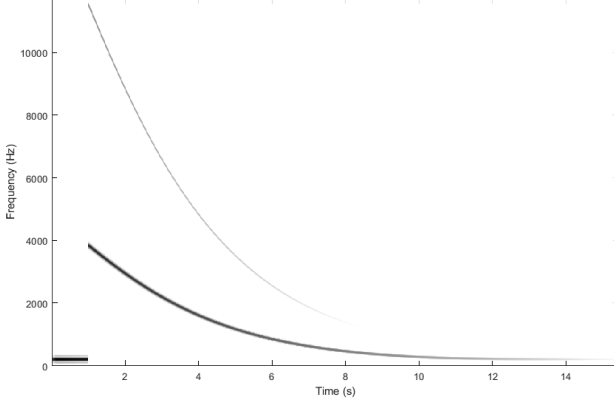

Figure 2: *Spectrogram of u for the single-degree-of-freedom system with a cubic spring term activated at $t = 1s$ with $\omega_1 = 300m^{-1/2}.s^{-1/2}$, initial conditions $u^0 = 1m$, $u^1 = 1m$.*

One can notice two phenomena related to the appearance of the non linear spring (see figure 2): the frequency of oscillation changes abruptly to an higher value then decreases and harmonic distortion appears (creation of the third harmonic). Thus, the frequency of non-linear modes varies with the amplitude of vibration of the spring (stiffness increases with amplitude, which is typical of springs of hardening type), and the waveform is no longer sinusoidal.

2.3. Effect of Collisions

The modeling of collisions with a rigid barrier may be written as the contact with a stiff unilateral non-linear spring (see figure 3), of restoring force $F_c = \frac{d\phi}{du}$, $\phi = \frac{K_c}{\alpha+1}[u]_+^{\alpha+1}$ ([16]).
With K_c the stiffness of the interaction, α the non-linear exponent, and $[u]_+ = (u + |u|)/2$ the positive part of u.
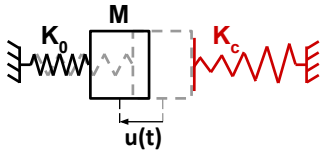

Figure 3: *Damped harmonic oscillator colliding with a barrier of stiffness K_c.*

$$\frac{\partial^2 u}{\partial t^2} = -\omega_0^2 u^n - \sigma_0 \frac{\partial u}{\partial t} - \frac{H(t - t_0)}{M}\frac{d\phi}{du} \quad (8)$$

We use the following scheme [16]:

$$\delta_{tt}u^n = -\omega_0^2 u^n - 2\sigma_0 \delta_t. u^n - \frac{H[n - \frac{t_0}{k}]}{M}\frac{\delta_{t-}\phi^{n+\frac{1}{2}}}{\delta_t. u^n} \quad (9)$$

with:

$$\phi^{n+\frac{1}{2}} = \frac{1}{2}\left(\phi(u^{n+1}) + \phi(u^n)\right) \quad (10)$$

It leads to the expression:

$$\mathcal{F}(r) = r + b + \frac{H[n - \frac{t_0}{k}]k^2}{M(1 + \sigma_0 k)}\frac{\Phi(r + a) - \Phi(a)}{r} = 0 \quad (11)$$

Given:
$r = u^{n+1} - u^{n-1}$,
$a = u^{n-1}$,
$b = (-2u^n + 2u^{n-1} + \omega_0^2 k^2 u_0^n)/(1 + \sigma_0 k)$

This equation can be solved using a Newton-Raphson algorithm at each time step.

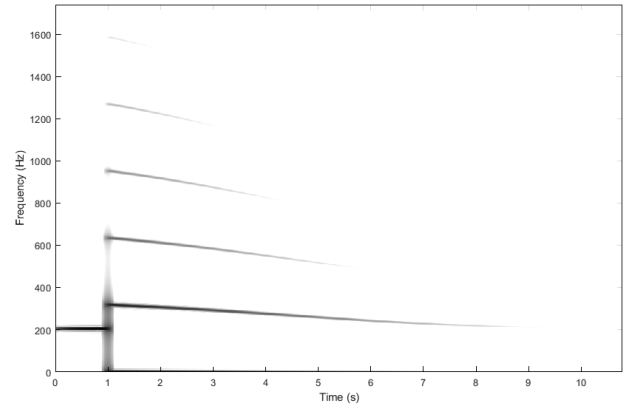We use the approximation $\frac{\Phi(r+a)-\Phi(a)}{r} \approx \Phi'(a)$ when $r < \epsilon$.

Figure 4: *Spectrogram of u for the single-degree-of-freedom system with a stiff unilateral non-linear spring appearing at $t_0 = 1s$. $K_c/M = 1.6 * 10^{10}m^{-1/2}.s^{-1/2}$, $\alpha = 1.9$ initial conditions $u^0 = 1m$, $u^1 = 1m$.*

The response for a unilateral non-linear spring is close to the classic non-linear spring (see figure 4). We observe a frequency-varying mode tending to the original mode as the amplitude tends to zero, and important harmonic distortion as the deformation of the waveform is abrupt.

To sum up, when a single-degree-of-freedom system collides with a non-resonant obstacle, it increases the frequency of its mode of vibration and creates harmonics. The frequency tends to its original value and the harmonic distortion disappears as the amplitude gets closer to zero.

As we switch the single-degree-of-freedom system to the stiff string, we can expect mode coupling when the descendant modes and their harmonics cross other modes of the structure, as we observe this kind of behavior on gongs and cymbals [19].

3. SPRINGS AND COLLISIONS ON A STIFF STRING

In this section, the linear model and the scheme used to synthesize realistic sounds of a stiff string is presented. Then, we study the

effects of linear and non-linear springs attached to the string on the frequency content of the samples in order to introduce how modes are impacted by perturbations. Finally, the collision model is implemented, and a description of the resulting morphology is presented.

3.1. Physical model of the stiff string and numerical scheme

The following partial differential equation describes the behavior of a stiff string subject to forces. This linear model does not take into account the variation of tension in the string (no pitch bending). it is commonly used for simulations and sound synthesis [20][21][18].

$$\frac{\partial^2 u}{\partial t^2} = c^2 \frac{\partial^2 u}{\partial x^2} - \kappa^2 \frac{\partial^4 u}{\partial x^4} - 2\sigma_0 \frac{\partial u}{\partial t} + 2\sigma_1 \frac{\partial^3 u}{\partial t \partial x^2} + \frac{1}{\rho S} \sum_m \delta(x - x_m) F_m \tag{12}$$

with:

· $u(x, t)$ the transversal motion of the string,

· $c = \sqrt{\frac{T}{\rho S}} = 404.02 m.s^{-1}$,

· $\kappa = \sqrt{\frac{E I_z}{\rho S}} = 1.297 m^2.s^{-1}$,

· $\delta(x)$ the Dirac function.

The signification and values of the parameters are defined in table1.

We can solve the equation using the following explicit finite difference scheme:

$$\delta_{tt} u = c^2 \delta_{xx} u - \kappa^2 \delta_{xxxx} u - 2\sigma_0 \delta_{t.} u + 2\sigma_1 \delta_{t_-} \delta_{xx} u + J_m . F_m \tag{13}$$

The previous equation can be displayed in a matrix form:

$$\bar{\bar{A}} \bar{u}^{n+1} = -\bar{\bar{B}} \bar{u}^n - \bar{\bar{C}} \bar{u}^{n-1} + \bar{J}_m F_m \tag{14}$$

with:

· h the grid spacing, chosen at the stability limit,
$h = \sqrt{\frac{(c^2 k^2 + 4\sigma_1 k + \sqrt{(c^2 k^2 + 4\sigma_1 k)^2 + 16\kappa^2 k^2})}{2}}$,

· k the time step interval, $k = 1/f_s$ with f_s the sampling frequency,

· $\delta_{xx} u = \frac{1}{h^2}(u_{l+1}^n - 2u_l^n + u_{l-1}^n)$,

· u_l^n the discretized value of $u(x,t)$ at the nth time step, and the lth step of the string,

· $\delta_{xxxx} u = \frac{1}{h^4}(u_{l+2}^n - 4u_{l+1}^n + 6u_l^n - 4u_{l-1}^n + u_{l-2}^n)$,

· $\delta_{t_-} u = \frac{1}{k}(u_l^n - u_l^{n-1})$,

· $\bar{e}_m = \begin{bmatrix} 0 & 0 & 0 & ... & 0 & 1 & 0 & ... & 0 \\ {}_1 & {}_2 & {}_3 & & {}_{i_{m-1}} & {}_{i_m} & {}_{i_{m+1}} & & {}_L \end{bmatrix}$

· $\bar{J}_m = \bar{e}_m^T / h$

· F_m is the scalar value of the force m.

The boundary conditions are simply supported at the end points of the domain $u(x = \{0, L\}, t) = 0$; $\frac{\partial^2 u}{\partial x^2}|_{(x=\{0,L\},t)} = 0$.

As excitation force, we use a simple model for a plucked string at $x = x_{ex}$:

$$F_e(t) = \begin{cases} A_f * (-\cos(\frac{\pi}{\Delta t} t) + 1) & if\ 0 \leq t < \Delta t \\ 0 & else \end{cases}$$

String:	
Diameter	$\phi = 1mm$
Length	$L = 0.5m$
Density	$\rho = 7800 kg.m^{-3}$
Young Modulus	$E = 210 GPa$
Tension	$T = 1000N$
Damping parameters:	$\sigma_0 = 0.05 rad.s^{-1}$
	$\sigma_1 = 0.002 rad.s^{-1}$
Sampling:	
Sampling frequency	$f_s = 176400 Hz$
Recording duration	$t_{rec} = 10s$
Excitation:	
Position	$x_{ex} = L/10$
Duration	$\Delta t_{ex} = 1ms$
Amplitude	$A_f = 100N$
Behavior:	
Maximum amplitude	$U_{max} = 0.0103m$
Resonance frequencies	$f_n = \frac{nc}{2L}\sqrt{1 + \left(\frac{\kappa \pi n}{c}\right)^2}$
	$f_1 = 410.7 Hz$

Table 1: Parameters used for the simulation

3.2. Spring on a stiff string

To observe the effects of a linear and a non linear spring on a stiff string, we use the string model presented eq. 12 with a linear and a cubic spring:

$$\frac{\partial^2 u}{\partial t^2} = c^2 \frac{\partial^2 u}{\partial x^2} - \kappa^2 \frac{\partial^4 u}{\partial x^4} - 2\sigma_0 \frac{\partial u}{\partial t} + 2\sigma_1 \frac{\partial^3 u}{\partial t \partial x^2} + \delta(x - x_s) F_s \tag{15}$$

with:

$$F_s = -\omega_0^2 u(x_s, t) - \omega_1^4 u(x_s, t)^3 \tag{16}$$

We use the following scheme (see eq.13 for the stiff string, eq. 7 for the non-linear spring):

$$\delta_{tt} u = c^2 \delta_{xx} u - \kappa^2 \delta_{xxxx} u - 2\sigma_0 \delta_{t.} u + 2\sigma_1 \delta_{t_-} \delta_{xx} u + J_s . F_s \tag{17}$$

with:

$$F_s = -\omega_0^2 u_{i_s} - \omega_1^4 (u_{i_s})^2 \mu_{t.} u_{i_s} \tag{18}$$

u_{i_s} is the element of the vector $\bar{u}$ at the point of application of the spring on the string (on the node $i = i_s$).

We observe a modification of the frequency of several modes of the string with a pure linear spring at $x = L/2$. These modifications remain constant as the signal evolves and follow a specific pattern (see figure 5): even harmonics remain approximately unchanged as they have a vibration node located at the application point of the spring, when odd harmonics get their frequency increased as they get stiffer around their vibration antinode. The frequency value of the odd harmonics gets greater with ω_0 but never exceed the next even harmonic, and the increase get lower as the rank of the harmonic get higher.

The quasi-harmonic string becomes in-harmonic, and those relatively low variations of the frequency content cause a categorical change of the perception: the system sounds like a linear plate or a shell.

For the cubic spring at $x = L/2$, the behavior is consistent with the previous observations: the even harmonics remain unchanged and
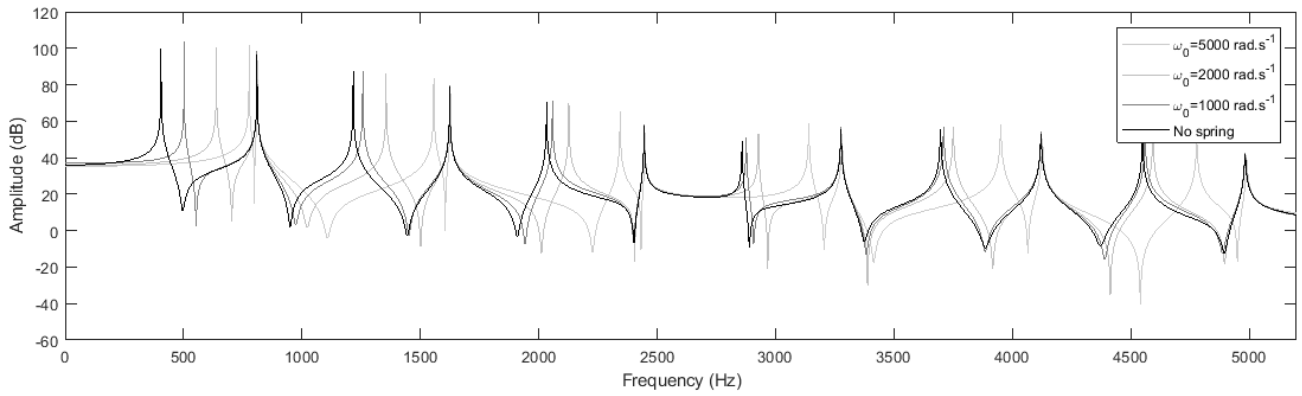
Figure 5: *FFT of the stiff string with a linear spring at $x = L/2$ for different values of ω_0.*
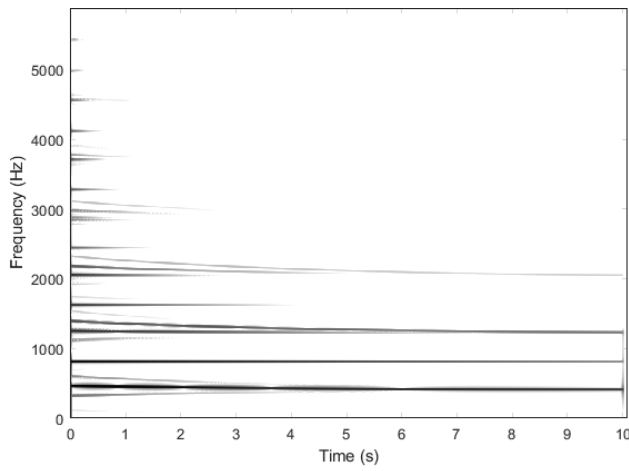

Figure 6: *Spectrogram of the stiff string with a cubic spring at $x = L/2$ for $\omega_1 = 300m^{-1/2}.s^{-1/2}$.*
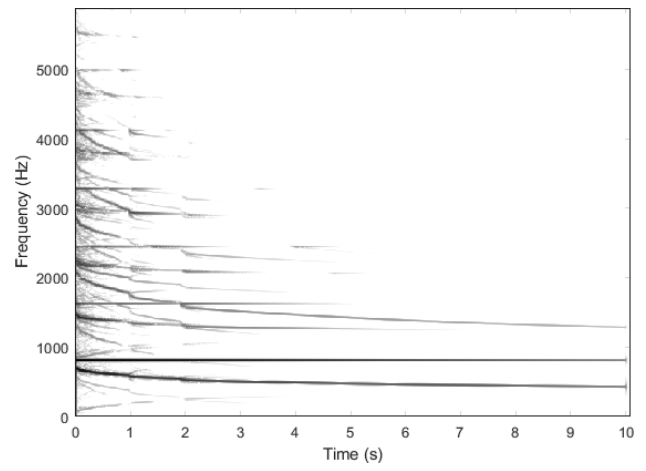

Figure 7: *Spectrogram of the stiff string with a cubic spring at $x = L/2$ for $\omega_1 = 1000m^{-1/2}.s^{-1/2}$.*

the frequency of the odd harmonics vary over time as the stiffness decrease with the amplitude (see figure 6).

But other effects caused by non-linearity appear. For $\omega_1 = 300m^{-1/2}.s^{-1/2}$, we can observe distinct frequency components around the original modes of the string, but in a large number due to harmonic distortion. Those new frequency components get closer to the original modes as the amplitude decrease over time. It is the same behavior that we observe on the single-degree-of-freedom system unless the modes are duplicated.

When the stiffness gets to high values (figure 7), a lot of components appear. This produces coupling between modes, resulting in fast variation of amplitude and frequency of several modes. It tends to chaotic behavior, creating a noisy-like signal at the beginning of the signal.

The perceived signal sounds like non-linear plates such as cymbals.

3.3. Stiff string colliding with a point rigid barrier

Considering the size of the article, we do not model the barrier as an object with its own dynamic but as a non-linear spring clamped

to the ground. We control the appearance of the barrier with the Heaviside function, and we manage to turn on the collision function when $u(x_c) < 0$ (x_c define the location of the barrier). In this case, the appearance of the obstacle does not create any transient behavior.

We use the collision model (eq. 8910) with the model of the stiff string (eq. 12 13).

$$\frac{\partial^2 u}{\partial t^2} = c^2 \frac{\partial^2 u}{\partial x^2} - \kappa^2 \frac{\partial^4 u}{\partial x^4} - \sigma_0 \frac{\partial u}{\partial t} + 2\sigma_1 \frac{\partial^3 u}{\partial t \partial x^2} + \delta(x - x_c)F_c \tag{19}$$

$$F_c = -\frac{H(t - t_0)}{\rho S} \frac{d\Phi}{du}\Big|_{(x=x_c,t)} \tag{20}$$

with $\Phi = \frac{K}{\alpha+1}[u_{i_c}]_+^{\alpha+1}$ and $[u]_+ = \frac{u+|u|}{2}$.

The corresponding scheme is presented bellow:

$$\delta_{tt}u = c^2\delta_{xx}u - \kappa^2\delta_{xxxx}u - 2\sigma_0\delta_t.u + 2\sigma_1\delta_{t_-}\delta_{xx}u + J_c.F_c \tag{21}$$
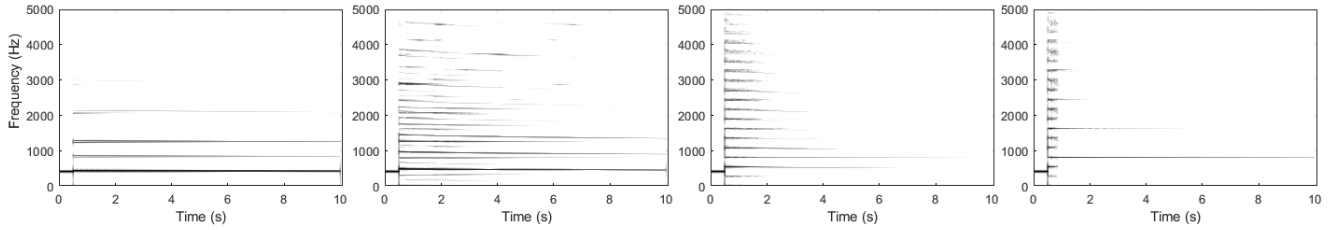
Figure 8: *Spectrogram of the stiff string ($u_l^0 = A_{max} sin(\pi \frac{lh}{L})$) colliding with a point rigid barrier ($\alpha = 1.6$) at $x = L/2$, from $t = 0.5s$, for different values of K_c. From the left: $K_c = 5 * 10^4 N.m^{-\alpha}$; $K_c = 5 * 10^5 N.m^{-\alpha}$; $K_c = 5 * 10^7 N.m^{-\alpha}$; $K_c = 5 * 10^8 N.m^{-\alpha}$.*

with:

$$F_c^n = -\frac{H[n - \frac{t_0}{k}]}{M} \frac{\delta_t - \phi^{n+\frac{1}{2}}}{\delta_t . u^n} \quad , \quad \phi^{n+\frac{1}{2}} = \frac{1}{2} \left(\phi(u_{i_c}^{n+1}) + \phi(u_{i_c}^n) \right)$$

(22)

u_{i_c} is the element of the vector $\bar{u}$ at the point of application of the collisions (on the node $i = i_c$).

the finite difference scheme at the local point of the collision (node i_c) gives the following non-linear equation:

$$\mathcal{F}(r) = r(1 + \sigma_0 k) + b + \frac{H[n - \frac{t_0}{k}]k^2}{\rho S h} \frac{\Phi(r + a) - \Phi(a)}{r} = 0$$

(23)

Given:
$r = u_{i_c}^{n+1} - u_{i_c}^{n-1}$,
$a = u_{i_c}^{n-1}$,
$b = < \bar{e}_c , (-2 - c^2 k^2 \delta_{xx} + \kappa^2 k^2 \delta_{xxxx} - 2\sigma_1 k \delta_{xx})\bar{u}^n >$
$+ < \bar{e}_c , (2 + 2\sigma_1 k \delta_{xx})\bar{u}^{n-1} >$

We use a Newton-Raphson algorithm to solve the scheme at this particular point.

4. SIGNAL MORPHOLOGIES DUE TO COLLISIONS ON STIFF STRINGS

4.1. Simulations and investigations

In order to make it easier to understand how the collisions modify the frequency response, we study the response of the system without excitation force with the following initial condition: $u_l^0 = U_{max} sin(\pi \frac{lh}{L})$ (see figure 9).
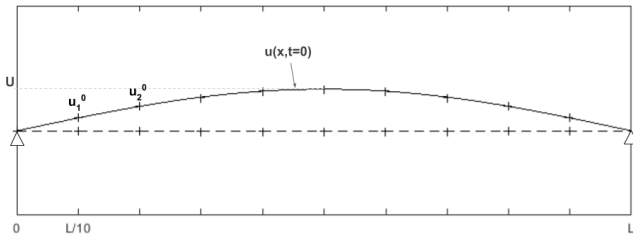

Figure 9: *Representation of the initial condition of the transverse displacement of the string.*

Here the string initially vibrates only on its first vibration mode until it collides with the barrier at $t_0 = 0.5s$. Then, we can observe a new distribution of the energy due to the frequency shift of the mode, harmonic distortion and mode coupling (figure 8). If we observe the left figure, we distinct clearly a frequency gap as the obstacle appears and a few harmonics of this mode are generated. Then, a few other modes of the string are excited due to mode coupling. This process expands itself as K gets higher. For a really stiff barrier, very high frequency components are generated (up to $25kHz$ for $K = 5 * 10^8 N.m^{-\alpha}$) causing important losses. Thus, all the components but the even harmonics disappear quickly, creating a vibration node at the location of the obstacle (here $L/2$).

The perceived sound is similar to a natural harmonic played on a guitar for high values of K. For low values of K, the string sounds like a bell as the barrier appear, and the frequency shift bring back the sound to a regular string.
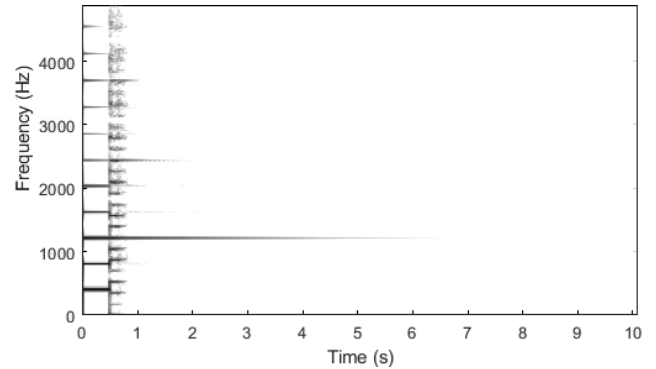

Figure 10: *Spectrogram of a plucked stiff string colliding with a point rigid barrier at $x = L/3$, from $t_0 = 0,5s$, for $K_c = 5 * 10^8 N.m^{-\alpha}$, and $\alpha = 1,6$.*

We study more specifically the cases that sound like a natural harmonic ($K \geq 1.10^8$) because it is a clearly identified type of interaction and we are able to specify a pattern corresponding to this behavior. The sounds generated for low values of K are peculiar and it is hard to recognize what is the source of it. We describe the pattern for the natural harmonic as following: if the considered mode of the string does not have a vibration node at the exact location of the obstacle, its frequency increases of a constant value ($\sim f_0/3$ for $x_c = L/2$) and a component appears in a symmetric way below with a lower amplitude. Harmonic distortion and mode coupling provoke the apparition of higher frequency components in the whole audible frequency band (and above) corresponding to other modes of the system {String + Rigid barrier}. These newly excited modes provoke the apparition of higher frequency compo-

nents themselves. This chain reaction induces important losses, and lasts for a short duration after which only the modes with a vibration node at the location of the obstacle remain.

From a perceptual point of view, the simultaneous presence of frequency components created by harmonic distortion and modes of the system create beats, roughness, and noisy-like signal at high frequency.

This pattern varies with the position of the obstacle. Generally, modes with a vibration node at the location of the obstacle keep their frequency unchanged but may undergo some variations of their amplitude (see the modes multiple of 3 for $x_c = L/3$ on figure 10). The modifications on the other modes depends on the ratio between the vibration amplitude and the proximity of the obstacle.

We introduce the scalar y, the transverse position of the rigid barrier. The expression of ϕ become $\phi = \frac{K_c}{\alpha+1}[u_{i_c} - y]_+^{\alpha+1}$.

Figure 11: *Spectrogram of a plucked stiff string colliding with a point rigid barrier at $(x = L/2; y = 0.065 * U(t_0 = 0.5s))$, from $t = 0.5s$, for $K_c = 5 * 10^8 N.m^{-\alpha}$, and $\alpha = 1.6$.*
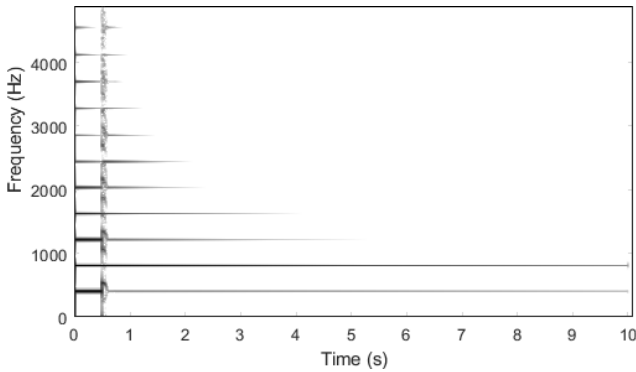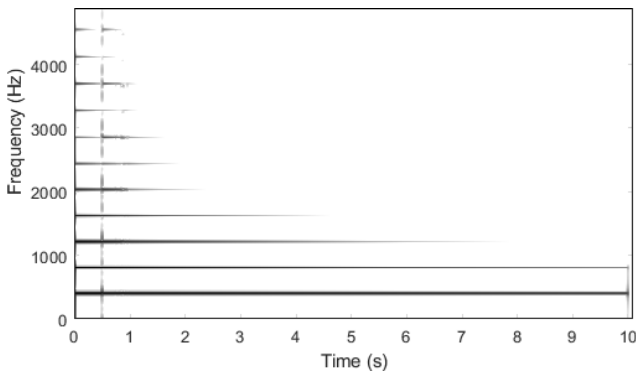

Figure 12: *Spectrogram of a plucked stiff string colliding with a point rigid barrier at $(x = L/2; y = 0.99 * U(t_0 = 0.5s))$, from $t_0 = 0.5s$, for $K_c = 5 * 10^8 N.m^{-\alpha}$, and $\alpha = 1.6$.*

As $y \neq 0$, the frequency components get back to the natural vibration modes of the string when the amplitude of u_{i_c} get below y. For instance, if $y = 0.065U(t_0)$ (with $U(t_0)$ the amplitude of u at the time of appearance of the obstacle), we observe a short
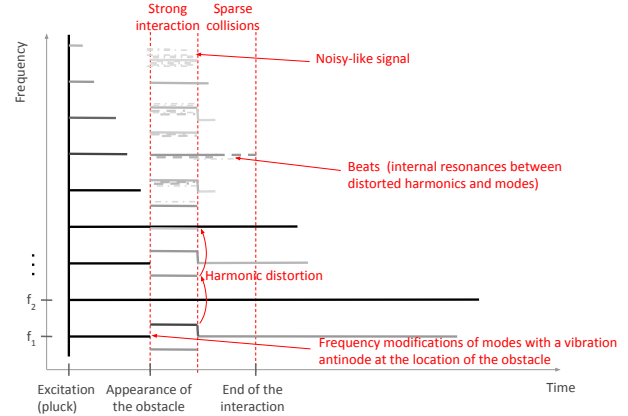

Figure 13: *Schematic Time-Frequency representation of a plucked stiff string colliding with a point rigid barrier at $(x = L/2)$.*

time of interaction ($\sim 0.1s$), then the string gets back to its regular vibrations with new initial conditions (see figure 11).

In the case of a really light touch ($y_0 = 0.99 * U(t_0)$), the pattern is close to disappear, but we can notice a very short apparition of new frequency components for $t = 0.5s$ and some slight harmonic distortion inducing mode coupling due to sparse collisions for $0.5s < t < 1s$ (see figure 12).

4.2. Towards a non-linear interaction invariant

Based on the previous considerations, we propose a description of the morphology of the signal resulting of the collisions between a stiff string and a stiff barrier. The highly non-linear nature of this interaction induces complex phenomena such as frequency shift, harmonic distortion and mode coupling.

Still, it is possible to define a pattern that describes the time-frequency content of the signal regarding the location and the nature of the obstacle (see figure 13). One can notice two different interaction phases:

· If the transversal position of the barrier is distinctly lower than the amplitude of vibration of the string, the interaction is strong. In this case, we observe important modifications of the modes' frequency and the generation of new partial tones due to harmonic distorsion and internal resonances. The partial tones are clearly distinguishable around the first modes, but it gets to noisy-like signal above the sixth mode.

· When the amplitude of vibration of the string is close to the transversal position of the barrier, we get to an other phase with sparse collisions. Here, we notice some harmonic distorsion that transfers energy from the first modes to the following ones, and it creates beats as the string is slightly inharmonic.

Hence, the transversal position of the obstacle has an influence on the duration of the strong interaction phase duration. The longitudinal position of the obstacle define which modes are modified. The material of the obstacle (stiffness and damping) will affect the energy distribution within the modes as the harmonic distorsion gets more important with the stiffness of the obstacle. This pattern is specific to a point rigid barrier, it may be of interest to expand it to a distributed contact model.

5. CONCLUSION

In this paper, we aimed at identifying sound morphologies due to nonlinear interactions between a stiff string and colliding objects. This is the first step towards the development of synthesis processes perceptually controlled. For that, we hypothesized that nonlinear interactions are perceived through morphological sound invariants. We based our investigations on a physical modeling of the interaction phenomena to synthesize realistic sounds with a perfect control of the experimental parameters. This led to an experimental sound data bank that we analyzed to observe the morphologies of the computed sounds in order to deduct typical signal behaviors. Eventually, we defined specific patterns linked to the nonlinear interaction that may be relevant perceptual cues for sound recognition. These patterns mainly rely on frequency shifts, harmonic distorsion and mode coupling that may be responsible for the perception of roughness occurring during the interaction.

The next step is to model the invariant from a signal point of view and to design a synthesis process with an intuitive control strategy. This signal model will be validated through formal listening tests, and will be possibly extended to more general sound textures.

6. REFERENCES

[1] William W Gaver, "What in the world do we hear?: An ecological approach to auditory event perception," *Ecological psychology*, vol. 5, no. 1, pp. 1–29, 1993.

[2] Stephen McAdams and Emmanuel Bigand, "Introduction to auditory cognition," 1993.

[3] James J Gibson, "The ecological approach to visual perception," 1979.

[4] William H Warren and Robert R Verbrugge, "Auditory perception of breaking and bouncing events: a case study in ecological acoustics.," *Journal of Experimental Psychology: Human perception and performance*, vol. 10, no. 5, pp. 704, 1984.

[5] Richard P Wildes and Whitman A Richards, "Recovering material properties from sound," *Natural computation*, pp. 356–363, 1988.

[6] Stephen Lakatos, Stephen McAdams, and René Caussé, "The representation of auditory source characteristics: Simple geometric form," *Perception & psychophysics*, vol. 59, no. 8, pp. 1180–1190, 1997.

[7] Mitsuko Aramaki, Mireille Besson, Richard Kronland-Martinet, and Sølvi Ystad, "Controlling the perceived material in an impact sound synthesizer," *IEEE Transactions on Audio, Speech, and Language Processing*, vol. 19, no. 2, pp. 301–314, 2011.

[8] Richard Kronland-Martinet, Sølvi Ystad, and Mitsuko Aramaki, "High-level control of sound synthesis for sonification processes," *AI & society*, vol. 27, no. 2, pp. 245–255, 2012.

[9] Simon Conan, Etienne Thoret, Mitsuko Aramaki, Olivier Derrien, Charles Gondre, Sølvi Ystad, and Richard Kronland-Martinet, "An intuitive synthesizer of continuous-interaction sounds: Rubbing, scratching, and rolling," *Computer Music Journal*, vol. 38, no. 4, pp. 24–37, 2014.

[10] Matthew D Hoffman and Perry R Cook, "Feature-based synthesis: Mapping acoustic and perceptual features onto synthesis parameters.," in *ICMC*. Citeseer, 2006.

[11] Mitsuko Aramaki, Richard Kronland-Martinet, Thierry Voinier, and Sølvi Ystad, "A percussive sound synthesizer based on physical and perceptual attributes," *Computer Music Journal*, vol. 30, no. 2, pp. 32–41, 2006.

[12] Mitsuko Aramaki, Charles Gondre, Richard Kronland-Martinet, Thierry Voinier, and Solvi Ystad, "Thinking the sounds: an intuitive control of an impact sound synthesizer," Georgia Institute of Technology, 2009.

[13] Etienne Thoret, Mitsuko Aramaki, Charles Gondre, Sølvi Ystad, and Richard Kronland-Martinet, "Eluding the physical constraints in a nonlinear interaction sound synthesis model for gesture guidance," *Applied Sciences*, vol. 6, no. 7, pp. 192, 2016.

[14] Maarten van Walstijn, Jamie Bridges, and Sandor Mehes, "A real-time synthesis oriented tanpura model," in *Proc. Int. Conf. Digital Audio Effects (DAFx-16)*, 2016, pp. 175–182.

[15] Stefan Bilbao et al., "Prepared piano sound synthesis," DAFx, 2006.

[16] Stefan Bilbao, Alberto Torin, and Vasileios Chatziioannou, "Numerical modeling of collisions in musical instruments," *Acta Acustica united with Acustica*, vol. 101, no. 1, pp. 155–173, 2015.

[17] Michele Ducceschi, "A numerical scheme for various nonlinear forces, including collisions, which does not require an iterative root finder," .

[18] Stefan Bilbao, *Numerical sound synthesis: finite difference schemes and simulation in musical acoustics*, John Wiley & Sons, 2009.

[19] KA Legge and NH Fletcher, "Nonlinearity, chaos, and the sound of shallow gongs," *The Journal of the Acoustical Society of America*, vol. 86, no. 6, pp. 2439–2443, 1989.

[20] Antoine Chaigne and Anders Askenfelt, "Numerical simulations of piano strings. i. a physical model for a struck string using finite difference methods," *The Journal of the Acoustical Society of America*, vol. 95, no. 2, pp. 1112–1118, 1994.

[21] Julien Bensa, Stefan Bilbao, Richard Kronland-Martinet, and Julius O Smith III, "The simulation of piano string vibration: From physical models to finite difference schemes and digital waveguides," *The Journal of the Acoustical Society of America*, vol. 114, no. 2, pp. 1095–1107, 2003.